

Rate of Quantal Excitation to a Retinal Ganglion Cell Evoked by Sensory Input

MICHAEL A. FREED

Department of Neuroscience, University of Pennsylvania, Philadelphia, Pennsylvania 19104-6058

Freed, Michael A. Rate of quantal excitation to a retinal ganglion cell evoked by sensory input. *J. Neurophysiol.* 83: 2956–2966, 2000. To determine the rate and statistics of light-evoked transmitter release from bipolar synapses, intracellular recordings were made from ON-alpha ganglion cells in the periphery of the intact, superfused, cat retina. Sodium channels were blocked with tetrodotoxin to prevent action potentials. A light bar covering the receptive field center excited the bipolar cells that contact the alpha cell and evoked a transient then a sustained depolarization. The sustained depolarization was quantified as change in mean voltage (Δv), and the increase in voltage noise that accompanied it was quantified as change in voltage variance ($\Delta\sigma^2$). As light intensity increased, Δv and $\Delta\sigma^2$ both increased, but their ratio held constant. This behavior is consistent with Poisson arrival of transmitter quanta at the ganglion cell. The response component attributable to glutamate quanta from bipolar synapses was isolated by application of 6-cyano-7-nitroquinoxaline (CNQX). As CNQX concentration increased, the signal/noise ratio of this response component ($\Delta v_{\text{CNQX}}/\Delta\sigma_{\text{CNQX}}$) held constant. This is also consistent with Poisson arrival and justified the application of fluctuation analysis. Two different methods of fluctuation analysis applied to Δv_{CNQX} and $\Delta\sigma_{\text{CNQX}}$ produced similar results, leading to an estimate that a just-maximal sustained response was caused by $\sim 3,700$ quanta s^{-1} . The transient response was caused by a rate that was no more than 10-fold greater. Because the ON-alpha cell at this retinal locus has $\sim 2,200$ bipolar synapses, one synapse released ~ 1.7 quanta s^{-1} for the sustained response and no more than 17 quanta s^{-1} for the transient. Consequently, within the ganglion cell's integration interval, here calculated to be ~ 16 ms, a bipolar synapse rarely releases more than one quantum. Thus for just-maximal sustained and transient depolarizations, the conductance modulated by a single bipolar cell synapse is limited to the quantal conductance (~ 100 pS at its peak). This helps preserve linear summation of quanta. The $\Delta v/\Delta\sigma^2$ ratio remained constant even as the ganglion cell's response saturated, which suggested that even at the peak of sensory input, summation remains linear, and that saturation occurs before the bipolar synapse.

INTRODUCTION

A central neuron encodes a stimulus by integrating transmitter quanta from multiple synapses. The rate at which quanta impinge on a neuron and the statistics of their arrival times determine the neuron's signal/noise ratio. For example, if quanta arrive with Poisson statistics, then the signal/noise ratio is proportional to the square root of the mean rate (Laughlin 1989). Mean rate and the statistics of arrival also determine how many quanta overlap temporally. This sets the instantaneous synaptic conductance that limits the linearity of summa-

tion. For example, if a large synaptic conductance saturates the driving force on the ions that provide the synaptic current, summation of quanta will be nonlinear (Freed et al. 1992; Koch et al. 1982; Martin 1955; Rall 1959). Despite their importance, quantal rate and the statistics of arrival are relatively unknown for central neurons during natural stimulation in an intact neural circuit.

In theory, rate and arrival statistics can be evaluated by counting quanta. This approach works in culture where a neuron receives quanta infrequently from a few synapses (Bekkers and Stevens 1995; Forti et al. 1997; Isaacson and Walmsley 1995; Liu and Tsien 1995). This approach has not proved feasible in intact neuronal circuits because quanta arrive from so many synapses at such high frequencies that individual quanta merge in the macroscopic voltage. An alternative approach has been to measure the mean and variance of the membrane voltage. If for different stimulus intensities, the ratio of these two measures is constant, then quantal arrival is consistent with Poisson statistics (Dodge et al. 1968; Katz and Miledi 1972). This has been found in a vertebrate circuit (cone to OFF bipolar cell) (Ashmore and Copenhagen 1983). Assuming that quantal arrival is indeed Poisson, measurements of mean and variance were used to calculate the quantal rate.

The present study used this method (measurement of voltage mean and variance) to estimate the mean rate and arrival statistics of quanta from bipolar cell synapses on the ON-alpha ganglion cell. For these cells in peripheral cat retina, the number of bipolar cell synapses is known (Kier et al. 1995). Thus from the total quantal rate, one can derive the quantal rate per bipolar synapse. Because the alpha cell also receives amacrine synapses, special precautions were taken to restrict the analysis to glutamate quanta from bipolar cells. This was done by applying a glutamate antagonist, CNQX, and analyzing only those components of the voltage mean and variance that were sensitive to this antagonist.

METHODS

Intracellular recording

Intracellular recordings were made from a superfused, flattened preparation of the mammalian retina (Dacey and Lee 1994; Jensen 1991). Experimental procedures were approved by the University of Pennsylvania Animal Care and Use Committee. A cat was anesthetized with ketamine (10 mg/kg im) and then pentobarbital sodium (50 mg/kg ip); an eye was removed, and the cat overdosed with pentobarbital. A 1×0.5 cm rectangle, which included the ventral retina, pigment epithelium, and sclera, was removed from the back of the eye and placed in a chamber on the stage of an upright microscope. The retina was superfused at 1–2 ml/min with tissue-culture medium

The costs of publication of this article were defrayed in part by the payment of page charges. The article must therefore be hereby marked "advertisement" in accordance with 18 U.S.C. Section 1734 solely to indicate this fact.

(minimal essential medium, Life Technologies, Rockville, MD), which was bubbled with a mixture of 95% oxygen and 5% carbon dioxide and heated to 34°C. Pharmacological agents were kept in an array of reservoirs, any of which could provide the superfusate. These agents were tetrodotoxin (TTX; Sigma, St. Louis, MO), 6-cyano-7-nitroquinoxaline (CNQX), L-(+)-2-amino-4-phosphonobutyric acid (L-AP4), bicuculline methobromide, strychnine, and *N*-(2,6-dimethylphenyl carbamoylmethyl) triethylammonium bromide (QX-314; RBI, Natick, MA). Electrodes were filled with 1% pyranine in 1 M KCl buffered with 0.1 M Tris (pH 7.3) and had tip resistances of ~ 100 M Ω .

To visualize ganglion cells, a few drops of 0.001% acridine orange were added to the superfusate. This dye was taken up by ganglion cell somas, causing them to fluoresce when excited with near-ultraviolet (UV) light (400–440 nm). An alpha cell was identified by its large soma, and the tip of a microelectrode was advanced until it touched the soma. The illumination was turned off, and the microelectrode was advanced to impale the cell. During recording, the pyranine diffused into the soma and dendrites, confirming the cell's identity.

To create visual stimuli, the filter cube used for epifluorescence microscopy was replaced by a mirror. This reflected light (from a 50-W mercury arc lamp) passed through a rectangular aperture, then through a series of neutral density and interference filters, and finally onto the retina. The stimulus comprised wavelengths of 650 ± 15 nm and, when controlled by an electromagnetic shutter, had a rise time of ~ 2 ms.

The stimulus intensity was $\sim 10^6$ photons $\mu\text{m}^{-2} \text{s}^{-1}$, which caused $\sim 5,000$ $\text{R}^* \text{s}^{-1} \text{rod}^{-1}$ (see calculation below) thus saturating the rod response (half saturation = $100 \text{R}^* \text{rod}^{-1} \text{s}^{-1}$) (Schneeweis and Schnapf 1999). The stimulus was presented for 1–2 s every 3–6 s. Between stimuli, the retina was in dim red light (termed "dark" in RESULTS; Kodak Safelight 1A, 440 nm cutoff), which allowed the rod response to recover. Recordings from retinal neurons under these conditions show that the initial 100–300 ms of the response has both rod and cone components; the remaining response has only a cone component (Freed et al. 1996).

Membrane potential was amplified using an electrometer and stored on a frequency modulated recorder. For fluctuation analysis, recordings were digitized at 1 kHz using an anti-aliasing filter (4-pole Bessel, $f_c = 500$ Hz). Electrode frequency response was measured by injecting white noise currents through the electrode into the bath, digitizing the resulting voltages at 10 kHz, and calculating the power spectrum. The frequency response was flat (± 3 dB) from 1 to 500 Hz. At 500 Hz, the power spectral density of ganglion cell voltage noise was down by 40 dB from its peak value (Fig. 7) and was thus negligibly affected by the electrode frequency response or by the anti-aliasing filter used for fluctuation analysis.

Digitized voltages were analyzed using a Macintosh computer and scientific analysis software (IGOR, Wavemetrics, Lake Oswego, OR). Intervals of voltage noise (~ 0.5 s long, as shown in Figs. 1, 2, and 5) were selected for analysis. The voltages within some of these intervals showed slight linear trends, due either to electrode drift or to a gradual decline of the cell's sustained depolarization (e.g., Fig. 9A). Before calculating variance and power spectra, the drift was corrected for by fitting a line to the voltages within the interval (regression fit) and subtracting this line from the voltages.

Calculating error due to dispersion of quantal size

Dispersion of quantal amplitude (i.e., variation around the mean) increases the variance of the voltage, causing an underestimate of quantal rate and an overestimate of quantal amplitude. Dispersion of quantal amplitude could come from several factors, including variation in vesicle size or filling, variation in the number of postsynaptic receptors, and electrotonic decay along the dendritic arbor (Bekkers et al. 1990; Frerking and Wilson 1996). For retinal ganglion cells, electrotonic decay is a small factor because their dendritic arbors are

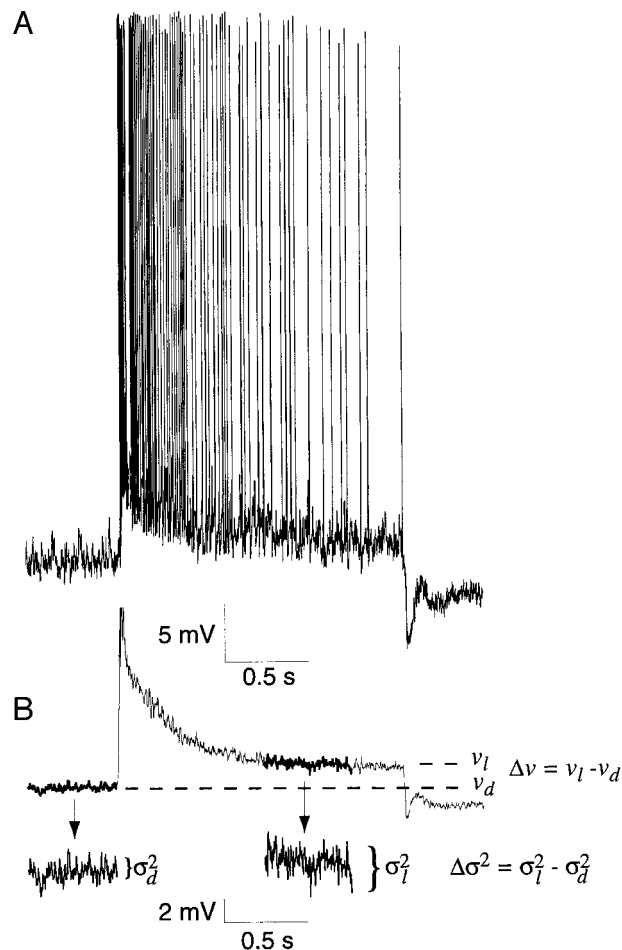


FIG. 1. Measuring Δv and $\Delta\sigma^2$. *A*: response to a bar of light. This cell had a low spike rate in the dark, but the dark rate varied among cells. *B*: during bath application of 20 nM TTX, Δv was measured as the difference between the mean voltage in the dark (v_d) and during the sustained depolarization (v_l); $\Delta\sigma^2$ was measured as the difference between the corresponding voltage variances (σ_d^2 and σ_l^2).

electrotonically compact (Coleman and Miller 1989; Freed et al. 1992; Taylor et al. 1995, 1996; Velte and Miller 1995). Apparently other factors are significant because the amplitudes of spontaneous excitatory postsynaptic currents (EPSCs) recorded from retinal ganglion cells in salamander have a 50% coefficient of variation ($\text{CV} = \text{SD}/\text{mean}$) (Taylor et al. 1995). Spontaneous PSCs in other neurons vary by a similar amount ($\text{CV} = 59\%$) (Frerking and Wilson 1996). If stimulus-evoked quanta vary to the same extent as spontaneous quanta, then fluctuation analysis would underestimate quantal rate and overestimate quantal amplitude by $(\text{CV})^2$ (Katz and Miledi 1972), $\sim 25\%$. Thus to correct for dispersion, the estimated quantal rate was multiplied by 1.25 and the estimated quantal amplitude was divided by the same factor.

Rate of photoisomerizations within the ganglion cell's receptive field center

Under RESULTS, I calculate the contribution of photon noise to the ganglion cell's light-evoked noise. This calculation requires an estimate for the total photoisomerization rate of all cones in the receptive field center. This calculation also requires a determination of whether the rods are saturated by the stimulus, which requires a similar estimation for a single rod. A cone outer segment is ~ 17 μm long (Steinberg and Wood 1974), and its absorptivity at the wavelength of

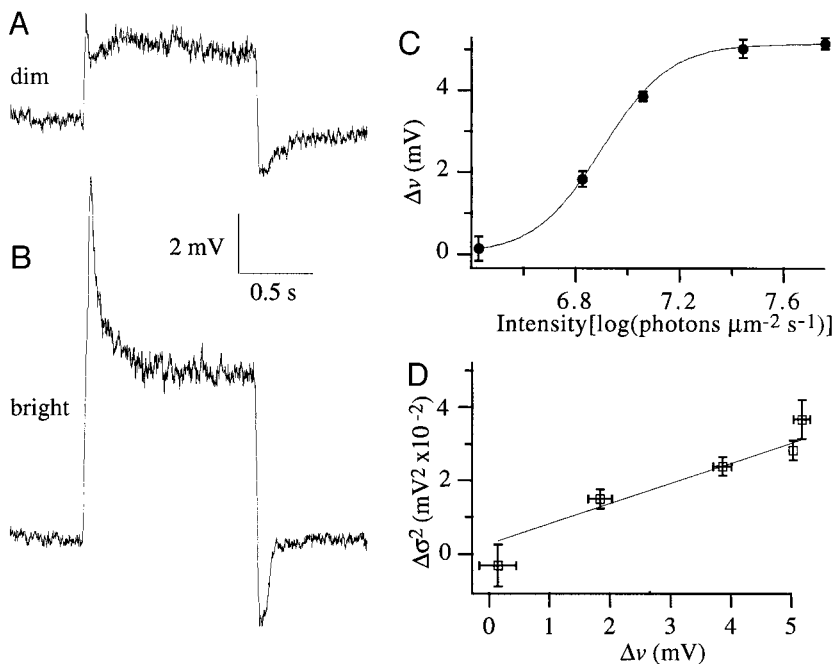


FIG. 2. As intensity increased, ratio of $\Delta\sigma^2$ to Δv remained constant. *A*: dim stimulus (6.3×10^6 quanta $\mu\text{m}^{-2} \text{s}^{-1}$) evoked a small, mostly sustained, depolarization with a small increase in voltage noise. *B*: bright stimulus (2.5×10^7 quanta $\mu\text{m}^{-2} \text{s}^{-1}$) evoked a large transient and sustained depolarization with larger increase in voltage noise. *C*: sustained response (Δv) saturated at high intensity (graph shows data from a single cell; error bars show SE; solid line is Naka-Rushton function). *D*: light-evoked change in variance ($\Delta\sigma^2$) vs. sustained response (from same cell) is fit by a regression line passing near the origin, demonstrating a constant ratio. This cell had a small $\Delta\sigma^2$; most other cells had a larger value ($0.11 \pm 0.3 \text{ mV}^2$).

peak sensitivity (556 nm) is $0.018 \mu\text{m}^{-1}$ (Harosi 1975). Thus the outer segment absorbance (absorptivity * length) equals 0.3 and its fractional absorbance [$1 - \log^{-1}(-\text{absorbance})$] equals 0.5. Given a photon efficiency of 0.7 (Dartnall 1968), each incident photon at the cone's peak wavelength causes $\sim 0.35 R^*$ (fractional absorbance * photon efficiency). The cone absorption at the stimulus wavelength (650 nm) is 0.158 times that at its peak sensitivity (Fig. 11 of Pflug et al. 1990), so R^* per incident photon is 0.055. The cross-sectional area of the cone outer segment is $\sim 3 \mu\text{m}^2$ (Steinberg and Wood 1974), and the stimulus intensity used for a just-maximal response was $\sim 10^6$ photons $\mu\text{m}^{-2} \text{s}^{-1}$, so photoisomerization rate per cone ($R^* \text{ photon}^{-1} * \text{cross-sectional area} * \text{intensity}$) was $\sim 1.7 \times 10^5 R^* \text{ s}^{-1} \text{ cone}^{-1}$. About 10° ventral to the area centralis, where the ON-alpha cells were recorded, there are $\sim 5,000$ cones mm^{-2} (Fig. 6 of Steinberg 1973). Thus the receptive field center, $\sim 300 \mu\text{m}$ in radius (personal observations; Peichl and Wässle 1979), encompasses $\sim 1,400$ cones. So the total photoisomerization rate ($R^* \text{ s}^{-1} \text{ cone}^{-1} * \text{number of cones}$) is $\sim 2 \times 10^8 R^* \text{ s}^{-1}$. A similar calculation for the rods, based on an outer segment length of $30 \mu\text{m}$, a cross-sectional area of $2 \mu\text{m}^2$, and a relative absorption ($\lambda_{650}/\lambda_{502}$) of 0.005 results in a photoisomerization rate per rod of $5,000 R^* \text{ s}^{-1}$. These calculations neglect self-screening, the waveguide properties of the cone inner segment, and tapetal reflectivity. But these are minor factors because, as shown in RESULTS, the calculated photon noise is six orders of magnitude less than the total light-evoked noise.

Rate of transmitter quanta from photoreceptors within the ganglion cell's receptive field center

In RESULTS, I calculate the contribution of quantal release from photoreceptors to the ganglion cell's light-evoked noise. This calculation requires the rate of transmitter quanta within the ganglion cell's receptive field center. In cat, each cone terminal has ~ 12 ribbon synapses (Sterling and Harkins 1990), and each rod terminal has 1 ribbon synapse (Rao et al. 1995). There are $\sim 5,000$ cones and $500,000$ rods per mm^2 (Steinberg and Wood 1974). Thus within the receptive field center (300 μm radius) there are $\sim 156,800$ photoreceptor synapses. The sustained release rate of a ribbon synapse in the dark is somewhere between 20 and 100 quanta s^{-1} (Ashmore and Copenhagen 1983; Rao et al. 1994; Rieke and Schwartz 1996). The lower of these two estimates is chosen to give an upper bound for

noise from quantal release. This results in a quantal rate for all photoreceptors within the receptive field center (n_{rc}) of 3×10^6 quanta s^{-1} .

RESULTS

After impalement a ganglion cell was observed for several minutes; if its dark potential was more negative than -50 mV and its action potentials were larger than 40 mV , it was selected for further study (Fig. 1A). Then, because action potentials obscured voltage noise, TTX (20 nM) was applied (Fig. 1B).

The stimulus was a bar $\sim 1 \times 0.6 \text{ mm}$, which covered the receptive field center and thus stimulated the bipolar cells presynaptic to the alpha cell. The intensity of the stimulus was incremented until, by visual inspection of the oscilloscope trace, the response was just maximal. The intensity for maximal response was $\sim 10^6$ photons $\mu\text{m}^{-2} \text{s}^{-1}$.

The response consisted of an initial transient depolarization followed by a sustained depolarization (Fig. 1B). The sustained response (Δv) was quantified by subtracting the mean in the dark from the mean during the sustained depolarization and averaged $3.5 \pm 0.4 \text{ mV}$ (mean \pm SE; $n = 13$ cells). The sustained response was accompanied by an increase in voltage noise. This noise increase ($\Delta\sigma^2$) was quantified by subtracting the variance in the dark from the variance during the sustained depolarization and averaged $0.11 \pm 0.03 \text{ mV}^2$.

Changing quantal rate did not alter $\Delta\sigma^2/\Delta v$

For quanta whose arrival times have Poisson statistics, the ratio of the voltage variance to the voltage mean ($\Delta\sigma^2/\Delta v$) is proportional to quantal amplitude (Katz and Miledi 1972). Thus changing quantal rate should not alter this ratio. The light-evoked quantal rate was increased by increasing stimulus intensity. This increased both $\Delta\sigma^2$ and Δv (Fig. 2, A-C). A plot of $\Delta\sigma^2$ versus Δv was linear and well fit by a regression line. The slope of this line varied from 6 to $33 \mu\text{V}$, but the line

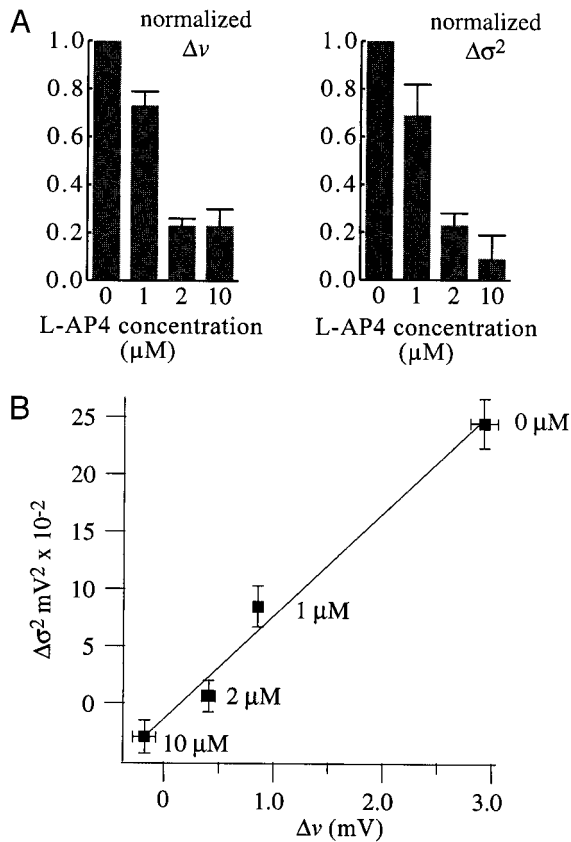


FIG. 3. As L-(+)-2-amino-4-phosphonobutyric acid (L-AP4) reduced Δv and $\Delta\sigma^2$, their ratio remained constant. *A*: quantification of L-AP4 effects (normalized to values at zero concentration; $n = 3$ cells). *B*: $\Delta\sigma^2$ vs. Δv from a single cell is fit by a regression line passing near the origin, demonstrating a constant ratio.

always crossed near the origin ($n = 5$ cells; Fig. 2*D*). Thus the ratio $\Delta\sigma^2/\Delta v$ was constant, consistent with quanta whose arrival times have Poisson statistics.

The light-evoked quantal rate was also changed pharmacologically to see again whether the ratio $\Delta\sigma^2/\Delta v$ remained constant. The light-evoked quantal rate was reduced by bath application of the glutamate agonist L-AP4, which reduces the light response of ON-bipolar cells (Slaughter and Miller 1981). L-AP4 was applied in concentrations from 1 to 10 μM , which

incrementally reduced Δv and $\Delta\sigma^2$ in the alpha cell (Fig. 3*A*). A plot of $\Delta\sigma^2$ versus Δv was linear and well fit by a regression line. The slope of this line varied from 38 to 89 μV , but the line always passed close to the origin ($n = 3$ cells; Fig. 3*B*). Thus the ratio $\Delta\sigma^2/\Delta v$ was again constant, consistent with quanta whose arrival times have Poisson statistics.

Changing quantal amplitude did not alter $\Delta v_{\text{CNQX}}/\Delta\sigma_{\text{CNQX}}$

For quanta whose arrival times have Poisson statistics, the signal/noise ratio ($\Delta v/\Delta\sigma$) is proportional to the square root of quantal rate (Katz and Miledi 1972). Thus changing quantal amplitude should not alter this ratio. To reduce the amplitude of quantal glutamate excitatory postsynaptic potentials (EPSPs) from bipolar cells, CNQX was added to the bath. Then the components of Δv and $\Delta\sigma$ sensitive to CNQX (Δv_{CNQX} and $\Delta\sigma_{\text{CNQX}}$) were analyzed to see whether the signal/noise ratio ($\Delta v_{\text{CNQX}}/\Delta\sigma_{\text{CNQX}}$) had changed.

The stimulus was presented repeatedly while the concentration of CNQX was increased stepwise (Fig. 4*A*). At each step, CNQX hyperpolarized the membrane potential and reduced the response amplitude. The variances before the response and during the sustained depolarization were both reduced, as was their difference, $\Delta\sigma^2$ (Fig. 4*B*). The same result was obtained from 4 ON-alpha ganglion cells (Fig. 5). Then Δv at the highest CNQX concentration was subtracted from the same measure at each CNQX concentration to give the component of Δv sensitive to CNQX (Δv_{CNQX}). The component of $\Delta\sigma^2$ sensitive to CNQX ($\Delta\sigma_{\text{CNQX}}^2$) was derived in similar fashion, and its square root gave $\Delta\sigma_{\text{CNQX}}$.

As CNQX concentration increased, Δv_{CNQX} and $\Delta\sigma_{\text{CNQX}}$ both decreased, and a plot of Δv_{CNQX} versus $\Delta\sigma_{\text{CNQX}}$ was linear and well fit by a regression line. The slope of this line averaged 6.6 ± 0.6 , and the line always crossed close to the origin ($n = 4$ cells; Fig. 6). Thus the ratio $\Delta v_{\text{CNQX}}/\Delta\sigma_{\text{CNQX}}$ was constant, consistent with quanta from bipolar cells arriving with Poisson statistics.

Total quantal rate from bipolar synapses

The total quantal rate arriving from all bipolar synapses to the ON-alpha cell during its sustained response was calculated by two methods. In the first method, the form of the quantum

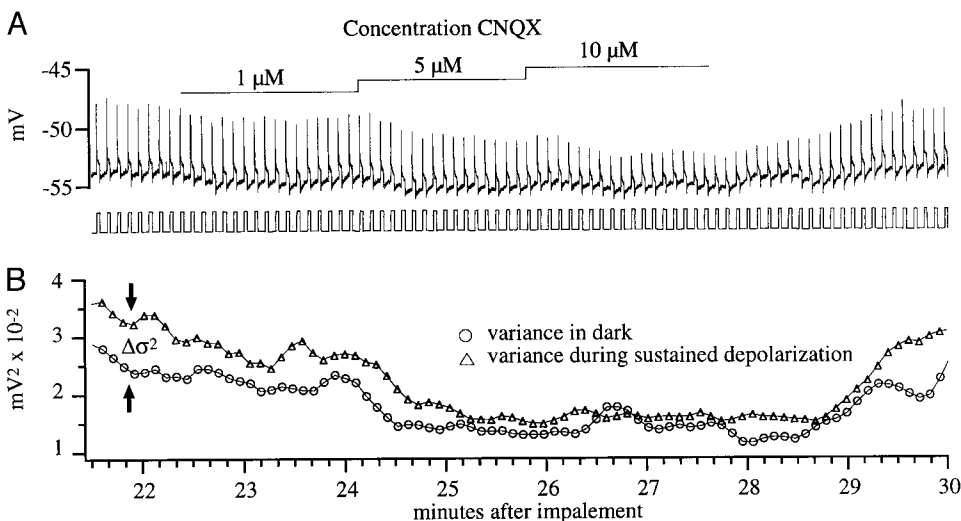


FIG. 4. Step increases in 6-cyano-7-nitroquinoxaline (CNQX) concentration caused step decreases in light-evoked variance ($\Delta\sigma^2$). *A*: penchart record of just-maximal responses to a repeated stimulus. Responses appear spikelike because of the slow time scale. *B*: 3-point running averages of the variance measured in the dark and during the sustained depolarization. Increasing CNQX concentration reduced the difference between these 2 measures, which is the light-evoked increase in variance ($\Delta\sigma^2$).

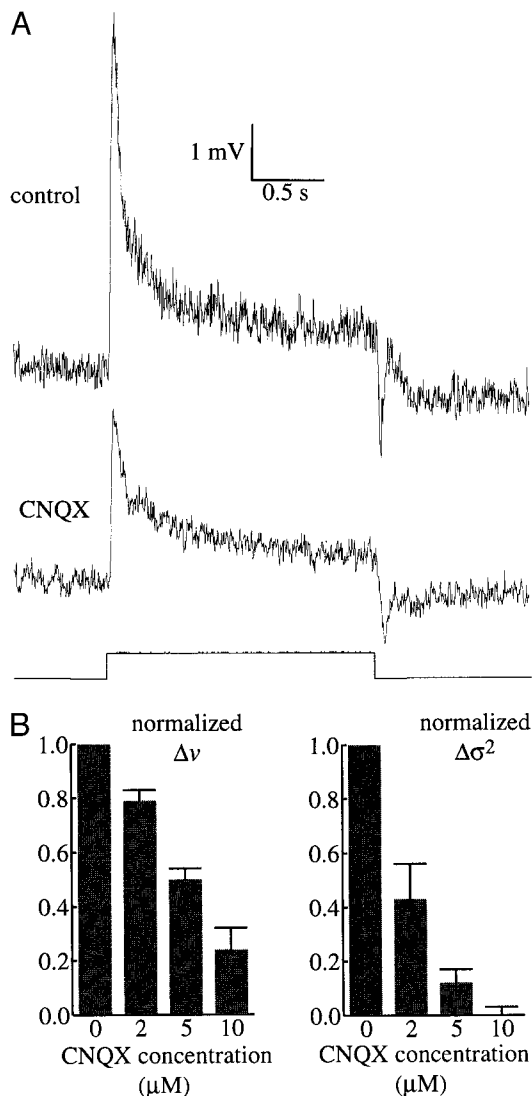


FIG. 5. CNQX reduced Δv and $\Delta\sigma^2$. A: responses for control and 10 μM CNQX. B: quantification of CNQX effects ($n = 4$ cells).

$f(t)$ was represented by the impulse response of a k -stage low-pass filter (Ashmore and Falk 1982; Taylor et al. 1996; Wong and Knight 1980)

$$f(t) = a(t/j\tau)^j e^{-t/\tau} \quad (1)$$

where $j = k - 1$, a is the peak amplitude of the event, and τ is a time constant. The sum of such events has a power spectrum of the form

$$F(f) = \frac{A}{[1 + (2\pi\tau f)^2]^k} \quad (2)$$

where A is the power spectral density at $F(0)$. To estimate the two parameters, k and τ , which describe the form of the quantum, the power spectrum of the CNQX-sensitive component of the noise was fit with Eq. 2 (Fig. 7). For different cells, k ranged from 0.7 to 1.1, and the time constant (τ) was 10 ± 3 ms. Because k approximated 1, the form of the quantum (Eq. 1) simplified to $f(t) = ae^{-t/\tau}$, which has a simple exponential decay with time constant τ . Also, the power spectrum (Eq. 2) simplified to a Lorentzian function. Given these simplifications, the quantal rate Δn could be estimated as

$$\Delta n = \frac{1}{2\tau} \left(\frac{\Delta v}{\Delta\sigma} \right)^2 \quad (3)$$

To evaluate Eq. 3 for bipolar synapses requires the ratio $\Delta v_{\text{CNQX}}/\Delta\sigma_{\text{CNQX}}$. This ratio was taken as the slope of the regression fit to the plots of $\Delta\sigma_{\text{CNQX}}$ versus Δv_{CNQX} (Fig. 6). The experimental values for this ratio and for τ (for each of 4 cells) were substituted into Eq. 3 and multiplied by 1.25 to adjust for dispersion of quantal amplitude (see METHODS). This yielded a rate for the sustained response of $3,400 \pm 1,000$ quanta s^{-1} .

The second method of calculating quantal rate made no assumptions about the shape of the event (Wong and Knight 1980). For the same four cells, the power spectrum of the CNQX-sensitive noise was inverse-Fourier transformed and then divided by its value at $t = 0$ to give the normalized autocorrelation function. The integral of this function estimated quantal duration T and averaged 16 ± 4 ms. The rate Δn was then calculated as

$$\Delta n = \frac{1}{T} \left(\frac{\Delta v}{\Delta\sigma} \right)^2 \quad (4)$$

This method, adjusted for dispersion of quantal amplitude, yielded a rate for the sustained response of $4,060 \pm 970$ quanta s^{-1} . Thus both methods, when applied to the same four cells, produced similar quantal rates. The calculations to follow use the average of the two methods, $3,700$ quanta s^{-1} .

In theory, the basal rate in darkness and the peak rate during the light-evoked transient could also be estimated because CNQX reduced mean voltage and variance in darkness and also reduced the transient (Figs. 4 and 5). However, these measures in darkness drifted too much over time to estimate the basal rate. Similarly, a single transient was too brief to allow its fluctuations to be averaged over time (fluctuation analysis), and the recording time (30 min) was too brief to allow averaging over transients (ensemble analysis). Nevertheless, because the largest transients were ~ 10 -fold larger than the sustained depolarization (Figs. 1B, 2B, 5A, and 9A), and because quantal summation during the transient is probably linear (see DISCUSSION), a 10-fold higher rate sets an upper bound of $37,000$ quanta s^{-1} .

Peak amplitude of quantal voltage

Given that the quantal voltage has a simple exponential decay, its peak amplitude a was estimated as

$$a = \frac{2\Delta\sigma^2}{\Delta v} \quad (5)$$

To calculate a , the values of $\Delta\sigma^2$ and Δv at 10 μM CNQX were subtracted from their control values, to derive the components of $\Delta\sigma^2$ and Δv attributable to glutamate release from bipolar cells ($\Delta\sigma_{\text{CNQX}}^2$ and Δv_{CNQX}). These components were substituted into Eq. 5. The result, divided by 1.25 to adjust for dispersion of quantal amplitudes, was 40 ± 5 μV .

This amplitude for an evoked quantum can be compared with the size of a spontaneous EPSC in other mammalian ganglion cells. This has a peak conductance of ~ 100 pS (Tian et al. 1998) and a decay time constant of ~ 1 – 6 ms (Protti et al. 1997; Tian et al. 1998); therefore the integral of its conductance is ~ 100 – 600 pS ms. Consider that the ON-alpha cell's

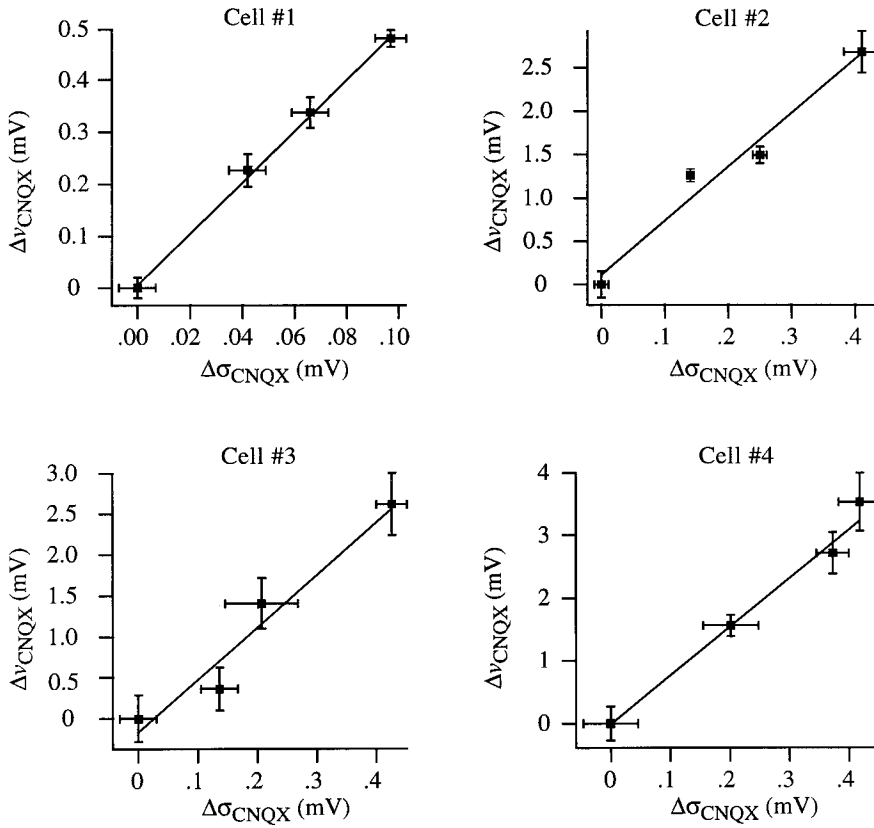


FIG. 6. As CNQX reduced response, the CNQX-sensitive component of this response retained a constant signal/noise ratio. Plots of the CNQX-sensitive component of the sustained response (Δv_{CNQX}) vs. the CNQX-sensitive component of light-evoked noise ($\Delta \sigma_{\text{CNQX}}$) are fit by regression lines passing close to the origin, demonstrating a constant ratio.

quantal conductance $g(t)$, in parallel with its input conductance G , and in series with the synaptic voltage E , causes a quantal voltage $f(t)$. The quantal voltage may outlast the quantal conductance, due to membrane capacitance, but the integrals of quantal voltage and quantal conductance are related by Ohm's law

$$\int g(t)dt = \frac{G}{E} \int f(t)dt \quad (6)$$

This equation assumes that the synaptic conductance is much smaller than the input conductance and thus that the synaptic

current-voltage relationship is linear (Martin 1955); the present study indicates that this assumption is reasonable (see DISCUSSION). Because the quantal voltage decays exponentially, its integral $\int f(t)$ is equal to $a\tau$ which, when substituted into Eq. 6, produces

$$\int g(t)dt = \frac{G}{E} a\tau \quad (7)$$

The decay time constant τ , taken from the power spectrum, averaged ~ 10 ms; synaptic voltage (E) is ~ 50 mV ($E_{\text{dark}} = -50$ mV and $E_{\text{glut}} = 0$ mV); input conductance (G) is ~ 8 nS

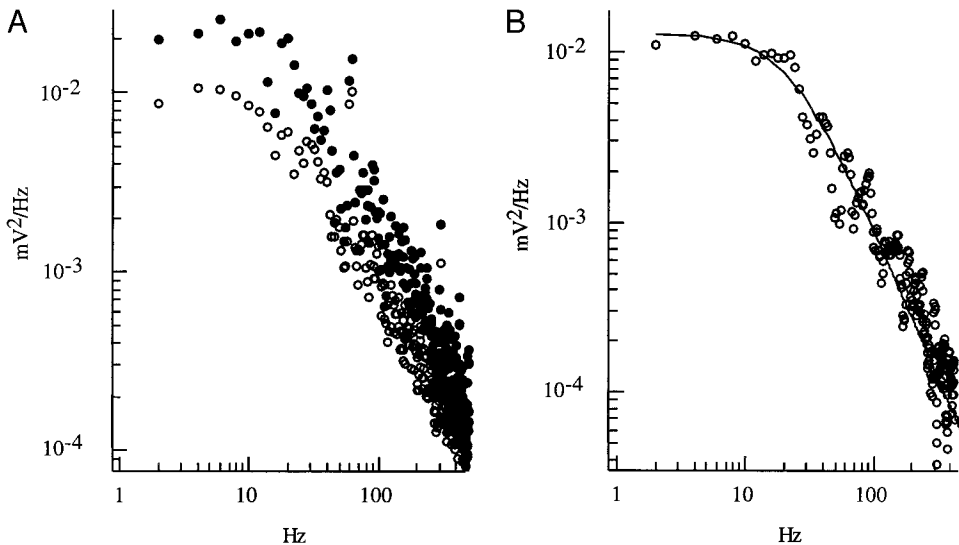


FIG. 7. A: power spectra of voltages during sustained depolarization (data from a single cell). ●, from control condition (average of 8 responses). ○, during CNQX (average of 25 responses; spectra from 0.1, 1, and 10 μM CNQX are combined). No smoothing. B: power spectrum of CNQX-sensitive quanta (difference between 2 spectra in A). Smoothing over 3 points below 100 Hz and over 5 points above 100 Hz. Solid curve is from Eq. 2.

(Freed et al. 1992). Thus the integral of the conductance is ~ 500 pS ms, similar to that calculated above from whole cell recordings (100–600 pS ms).

The ON-alpha cell's macroscopic light-evoked conductance G_{light} can be calculated as the product of quantal rate and the quantal conductance integral

$$G_{\text{light}} = \Delta n \int g(t) dt \quad (8)$$

Using the values of $3,700$ quanta s^{-1} and 500 pS ms, the macroscopic conductance is 1.9 nS, close to the approximate 1 -nS conductance for a sustained depolarization measured in a previous study (Freed et al. 1991, 1992).

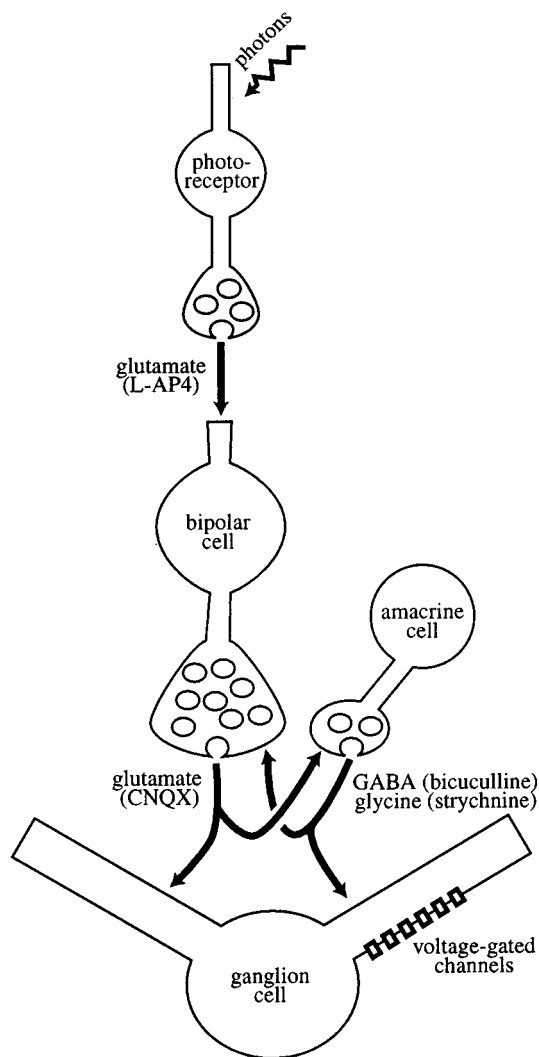


FIG. 8. Main sources of noise in ON-alpha ganglion cell. CNQX-sensitive noise in the ON-alpha cell results from bipolar cell quanta but might also come from several other sources: 1) CNQX might antagonize bipolar release onto the amacrine cell, which could reduce the rate of amacrine release onto the ON-alpha cell or, via feedback synapses, increase the rate of bipolar cell release onto the ON-alpha cell; 2) photon noise and photoreceptor release might modulate bipolar release; and 3) bipolar cell release might modulate voltage-gated channels in the ON-alpha cell. Despite these possible complications, bipolar release into the ON-alpha appears to be the source of CNQX-sensitive noise.

Possible contributions of upstream and downstream noise sources to $\Delta\sigma^2$

Conceivably, noise sources upstream of the bipolar synaptic terminal might modulate its vesicular release (Fig. 8). Also, noise sources downstream of the bipolar terminal might be modulated by bipolar release. Either upstream or downstream modulation would add to the ganglion cell's $\Delta\sigma^2$. Therefore the contributions of the main upstream and downstream noise sources were examined.

LAMP NOISE. Light source intensity fluctuated due to instability of the power supply voltage (signal/noise ratio ≈ 50). If this added to the light-evoked noise increase, then it would decrease the signal/noise ratio of the sustained response. However, light ON increased noise in ON-alpha cells (Fig. 1) by the same amount as light OFF increased noise in OFF-alpha cells. Consequently, their signal/noise ratios were not significantly different ($\Delta v/\Delta\sigma = 16 \pm 2$ for 4 OFF cells and 15 ± 2 for 13 ON cells). Because $\Delta v/\Delta\sigma$ was independent of whether the stimulus was on or off, fluctuations in lamp intensity could not have contributed significantly to $\Delta\sigma^2$.

PHOTON NOISE. A single photon absorbed by a rod can affect spiking in a profoundly dark-adapted ganglion cell (Barlow et al. 1971; Mastrorade 1983). This suggests that at any light level, a photoreceptor is capable of transmitting photon noise to the ganglion cell. However, in the dark, photon noise was negligible, and during the bright stimulus, the rod response was saturated (see METHODS). Thus virtually all photon noise in the alpha cell came from cones.

The cone contribution to $\Delta\sigma^2$ was calculated by rearranging Eq. 4

$$\Delta\sigma_{R^*}^2 = \frac{\Delta v^2}{n_{R^*} T_{R^*}} \quad (9)$$

where $\Delta\sigma_{R^*}^2$ is the light-evoked change in variance due to photon absorptions; Δv is the sustained response; n_{R^*} is the photoisomerization rate; and T_{R^*} is the photon event duration. The total rate n_{R^*} for cones within the receptive field center is $\sim 2 \times 10^8 R^* s^{-1}$ (see METHODS) and $\Delta v = 3.5$ mV (see above). T_{R^*} is ~ 100 ms (Baylor et al. 1984). Because T_{R^*} is longer than the time constants of other retinal neurons, it is not lengthened by transmission to the alpha cell. Thus $\Delta\sigma_{R^*}^2$ is calculated to be $\sim 6 \times 10^{-7}$ mV². Compared to the alpha cell's light-evoked increase in variance ($\Delta\sigma^2 \approx 10^{-1}$ mV²), this is negligible. Had rods been included in the preceding calculation, the photon contribution to $\Delta\sigma^2$ would have been even smaller. Thus the contribution of photon noise to $\Delta\sigma^2$ was insignificant.

NOISE FROM PHOTORECEPTOR RELEASE UPON BIPOLAR CELLS. Light reduces quantal release by photoreceptor terminals. Because bright light also reduces noise in bipolar cells (including those types that contact the ON-alpha cell) (Nelson et al. 1981; R. Taylor, personal communication), quantal release from photoreceptors is apparently the bipolar cell's main noise source. Thus photoreceptor release would contribute indirectly to the ON-alpha cell's $\Delta\sigma^2$. Because stimulus rate (~ 0.3 Hz) was low enough to allow rods responses to recover (see METHODS), the rods must repolarize between stimuli and resume quantal release. Thus rods would contribute to quantal noise as well as cones. Therefore the total contribution of both photoreceptors was calculated by rearranging Eq. 3

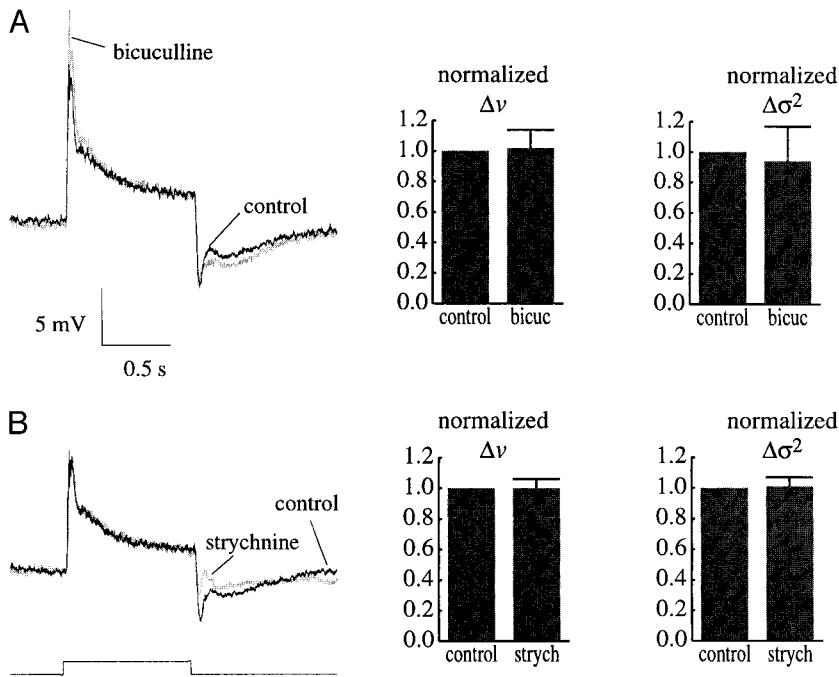


FIG. 9. GABA and glycine antagonists had insignificant effects on Δv and $\Delta\sigma^2$. *A*: effects of bicuculline (20 μM ; $n = 4$ cells). *B*: effects of strychnine (0.5 μM ; $n = 3$ cells).

$$\Delta\sigma_{rc}^2 = \frac{\Delta v^2}{2n_{rc}\tau_{rc}} \quad (10)$$

where $\Delta\sigma_{rc}^2$ is the light-evoked change in variance contributed by rod and cone quanta and n_{rc} is the release rate ($\sim 3 \times 10^6$ quanta s^{-1} ; see METHODS). Because each quantal event is brief enough to be lengthened by the alpha cell's membrane capacitance, τ_{rc} is the same as the membrane time constant (~ 10 ms, as confirmed above by power spectra). Thus $\Delta\sigma_{rc}^2$ is $\sim 10^{-4}$ mV^2 . This is larger than the variance due to photon absorption, but still negligible compared with the alpha cell's total $\Delta\sigma^2$ ($\approx 10^{-1}$ mV^2).

NOISE FROM AMACRINE RELEASE ONTO THE GANGLION CELL. Quanta released by bipolar cells might modulate the amacrine cell's release and thus contribute indirectly to the ON-alpha cell's $\Delta\sigma^2$. Most amacrine cells employ GABA or glycine as a transmitter (Marc et al. 1995; Strettoi and Masland 1996), and the postsynaptic ON-alpha cell has GABA_A and glycine receptors (but not GABA_B or GABA_C receptors) (Cohen et al. 1994). The contributions of GABA and glycine to $\Delta\sigma^2$ were evaluated (in separate experiments) by adding their respective antagonists bicuculline and strychnine to the bath in concentration known to effectively block the respective currents in the ON-alpha cell (Cohen et al. 1994). Bicuculline (20 μM) increased the transient, and strychnine (0.5 μM) increased basal noise, but neither significantly affected Δv or $\Delta\sigma^2$ (Fig. 9). Apparently, under the conditions of the main experiment, neither GABA nor glycinergic amacrine cells add to $\Delta\sigma^2$.

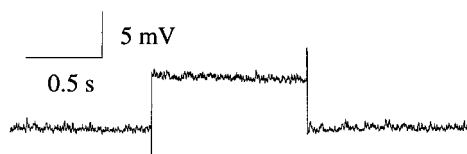


FIG. 10. Injecting current (50 pA) into cell during bath application of TTX caused sustained depolarization but did not increase voltage noise.

NOISE FROM VOLTAGE-GATED CHANNELS. Although TTX blocked the alpha cell's voltage-gated sodium channels, it seemed possible that the sustained depolarizing response might activate other types of voltage-gated channel (K^+ , Ca^{2+}) that might contribute to $\Delta\sigma^2$. Therefore steps of positive current (50–100 pA) were injected into three cells to cause depolarizations similar in amplitude to Δv (3–10 mV; Fig. 10). For all three cells, the light-evoked variance was not significantly different from zero (Student's *t*-test; $P > 0.65$). Thus in the presence of TTX, voltage-gated channels do not add to $\Delta\sigma^2$.

DISCUSSION

The key conclusion is that a stimulus of just-maximal intensity to the ganglion cell's receptive field center evokes sustained release from bipolar cells of $\sim 3,700$ quanta s^{-1} . Before discussing the implications of this conclusion, it is necessary to treat the main assumptions on which it rests.

The conclusion derives from standard fluctuation analysis, which assumes quanta arrive with Poisson statistics (Dodge et al. 1968; Katz and Miledi 1972). If arrival is Poisson, then the variance/mean ratio remains constant as the rate changes. This held true when quantal rate increased with increasing stimulus intensity (Fig. 2*D*), and when quantal rate decreased with L-AP4 (Fig. 3*B*). If arrival is Poisson, then the signal/noise ratio remains constant as quantal amplitude changes. This also held true when quantal amplitude decreased with CNQX antagonism (Fig. 6). Poisson statistics are found where spontaneous quanta arrive at low rates on the ganglion cell (5–200 s^{-1}) (Gao et al. 1997; Matsui et al. 1998; M. Tachibana, personal communication), and the present findings suggest that, as the rate rises due to stimulation, arrival statistics remain constant. Poisson statistics have also been found by measuring the variance/mean ratio for the OFF-bipolar cell at very high stimulated rates (9,200 quanta s^{-1}) (Ashmore and Copenhagen 1983).

Constant ratios of variance/mean and signal/noise could also

be consistent with a *doubly* Poisson process (Teich 1981). This would result if Poisson noise sources *upstream* of the bipolar cell modulated the bipolar cell's quantal release. One consequence of such modulations would be an increase in light-evoked noise in the ON-alpha cell. Yet, negligible additions to $\Delta\sigma^2$ were found from the main upstream sources (photon absorptions, photoreceptor transmitter release, and amacrine cells) implying that these do not modulate the bipolar cell's transmitter release. Furthermore, were the bipolar cell's release modulated by upstream noise, the power spectrum of the ganglion cell's voltage noise would be attenuated at lower frequencies and peak at higher frequencies (Wong and Knight 1980), but this was not observed (Fig. 7B).

Doubly Poisson statistics might also result if bipolar cell release modulated Poisson noise sources *downstream*, again increasing light-evoked noise. Normally, sodium channels would be activated by the sustained depolarization and would provide a large source of downstream noise. However, these were blocked with TTX, and injecting depolarizing current ruled out possible contributions from other voltage-activated channels. Amacrine cell release on the ON-alpha cell might be modulated by bipolar cells, but, as evident in the null effects of bicuculline and strychnine, amacrine cells contribute insignificantly to the ON-alpha cell's sustained light-evoked noise.

The present analysis assumes that CNQX affects noise solely by antagonizing glutamate quanta released by bipolar cells onto the ON-alpha cell. CNQX probably also antagonizes glutamate quanta released by bipolar cells onto amacrine cells. This would reduce both amacrine release onto the ON-alpha cell and, because amacrine cells feed back on the bipolar cell, would increase the rate of bipolar release onto the ON-alpha cell (Fig. 8). Because quantal rate is proportional to the square of the signal/noise ratio (Eq. 3), an alteration in rate would alter the signal/noise ratio. Yet no such alteration was observed. Because quantal rate was estimated from this signal/noise ratio, any contribution of amacrine cells to this estimate was negligible.

The analysis also assumes that the ON-alpha cell sums quanta linearly. This is consistent with finding that as quantal rate increased, the variance/response ratio remained constant (Fig. 2D). The variance/response ratio is proportional to the amplitude of the quantal voltage (Eq. 5), and thus the quantal voltage must have been constant. If summation were nonlinear, increasing quantal rates would have caused successively smaller quantal voltages. Finally, fluctuation analysis yielded a value for both the quantal and the macroscopic conductances that are close to those measured directly. Thus 3,700 quanta s^{-1} seems a reasonably good estimate, and I now consider some implications.

Release rate from a single bipolar cell synapse

The sustained release rate evoked by light from a single bipolar cell synapse can be obtained by dividing the total quantal rate (3,700 quanta s^{-1}) by the number of bipolar synapses on the ON-alpha ganglion cell. This number can be extrapolated from the smaller ON-alpha cells in the area centralis that have 550 synapses (Freed and Sterling 1988) to the larger ON-alpha cells of the present study recorded at 10° eccentricity. The density of bipolar synapses on the membrane is constant, and cells at 10° have fourfold greater membrane

area (Kier et al. 1995), so they should have $\sim 2,200$ synapses. Thus the sustained rate at a single bipolar synapse is ~ 1.7 quanta s^{-1} . Given that the alpha cell's transient depolarization is no more than 10-fold larger than the sustained depolarization, an upper bound for the transient release rate is ~ 17 quanta s^{-1} . This number seems reasonable given that peak rates >20 quanta s^{-1} have been reported for other ribbon synapses by capacitance measurements (Rieke and Schwartz 1996; von Gersdorff et al. 1996) and by noise analysis (Ashmore and Copenhagen 1983).

Mechanism of linear summation

At low to moderate stimulus intensities, a ganglion cell's response is proportional to stimulus flux (Barlow 1953; Cleland and Enroth-Cugell 1968). The mechanisms for this linear summation have not been established. For a ganglion cell to linearly sum the voltages generated by successive or adjacent quanta, the quantal conductance must be small relative to the dendritic input conductance (Freed et al. 1992; Koch et al. 1982; Martin 1955; Rall 1959). Otherwise the voltages generated by each successive or adjacent quantum would be smaller. Also, the quantal EPSP must be small relative to the potential difference driving the permeant ions, otherwise each quantum would reduce the driving force for generating successive currents.

A multicompartiment model of the ON-alpha cell suggested that, if the light-evoked conductance applied by a single synapse were low enough (~ 100 pS), summation would be linear (Freed et al. 1992). The present results and recordings from other mammalian ganglion cells indicate a peak quantal conductance of ~ 100 pS (Tian et al. 1998); thus if quanta were to overlap in time, the total synaptic conductance would exceed 100 pS, causing nonlinear summation. However, 1.7 quanta s^{-1} implies ~ 0.03 quanta per integration interval ($T = 16$ ms). It follows from Poisson statistics that quanta overlap rarely ($P = 0.0004$). Even at the highest rate (17 quanta s^{-1}) during the transient, quanta would overlap rarely ($P = 0.036$).

Other mechanisms to preserve ganglion cell linearity have been described. One mechanism uses the nonlinear voltage dependency of the *N*-methyl-D-aspartate (NMDA) current to cancel saturation of the non-NMDA current (Mittman et al. 1990). Another mechanism uses voltage-gated conductances to clamp the membrane potential, preventing saturation of the synaptic driving force (Diamond and Copenhagen 1995). If this mechanism were to serve the ON-alpha cell, then TTX, by relieving this clamp, should augment its response. TTX did augment the transient depolarization but actually reduced the sustained depolarization (Fig. 1), suggesting that this mechanism is limited to the transient.

Mechanism for saturation

At higher stimulus intensity, the alpha cell's response begins to saturate (Fig. 2C). This saturation could occur anywhere between the photoreceptor and, where voltages were recorded, the alpha soma (Fig. 8). If saturation occurred at the ON-alpha cell dendrites, due to exceeding the synaptic conductance consistent with linear summation, then the quantal EPSP amplitude would be reduced. Yet, during saturation, the alpha cell's variance/mean ratio remains constant (Fig. 2D). Because this

ratio is proportional to quantal amplitude (Eq. 5), this constancy implies that quantal EPSP amplitude must have been constant. Thus saturation apparently is caused by a curtailing of quantal release from bipolar synapses and could originate anywhere upstream of these synapses.

Natural quantal rates on other neurons

Where the natural quantal rate impinging on a single neuron has been measured, it appears to be low. In the present case, a mammalian ganglion cell during visual stimulation receives $\sim 3,700$ quanta s^{-1} from $\sim 2,200$ synapses distributed across the dendritic tree. This rate is low in that only ~ 60 quanta overlap temporally during the sustained depolarization ($3,700$ quanta $s^{-1} * 16$ ms). The low rate plus the modest quantal conductance reduce interactions between quanta, allowing their linear summation. Similarly, a spinal interneuron during natural patterned motor activity receives ~ 100 quanta s^{-1} or only about five overlapping quanta from an unknown number of synapses (Raastad et al. 1996). However, the spinal neuron differs in that individual quantal conductances are large compared with the input conductance and thus could cause brief, but significant, nonlinearity (Raastad et al. 1998).

The author is grateful for thoughtful discussions with R. Nelson and R. Smith. Special thanks to P. Sterling for carefully reading this manuscript and making excellent suggestions.

This work was supported by National Eye Institute Grant R01 EY-11138.

Received 10 May 1999; accepted in final form 18 January 2000.

REFERENCES

- ASHMORE, J. F. AND COPENHAGEN, D. An analysis of transmission from cones to hyperpolarizing bipolar cells in the retina of the turtle. *J. Physiol. (Lond.)* 340: 569–597, 1983.
- ASHMORE, J. F. AND FALK, G. An analysis of voltage noise in rod bipolar cells of the dogfish retina. *J. Physiol. (Lond.)* 332: 273–297, 1982.
- BARLOW, H. Summation and inhibition in the frog's retina. *J. Physiol. (Lond.)* 119: 69–88, 1953.
- BARLOW, H. B., LEVICK, W. R., AND YOON, M. Responses to single quanta of light in retinal ganglion cells of the cat. *Vision Res.* 3: 87–101, 1971.
- BAYLOR, D. A., NUNN, B. J., AND SCHNAPF, J. L. The photocurrent, noise and spectral sensitivity of rods of the monkey *Macaca fascicularis*. *J. Physiol. (Lond.)* 357: 575–607, 1984.
- BEKKERS, J. M., RICHERSON, G. B., AND STEVENS, C. F. Origin of variability in quantal size in cultured hippocampal neurons and hippocampal slices. *Proc. Natl. Acad. Sci. USA* 87: 5359–5362, 1990.
- BEKKERS, J. M. AND STEVENS, C. F. Quantal analysis of EPSCs recorded from small numbers of synapses in hippocampal cultures. *J. Neurophysiol.* 73: 1145–1156, 1995.
- CLELAND, B. G. AND ENROTH-CUGELL, C. Quantitative aspects of sensitivity and summation in the cat retina. *J. Physiol. (Lond.)* 198: 17–38, 1968.
- COHEN, E. D., ZHOU, Z. J., AND FAIN, G. L. Ligand-gated currents of alpha and beta ganglion cells in the cat retinal slice. *J. Neurophysiol.* 72: 1260–1269, 1994.
- COLEMAN, P. A. AND MILLER, R. F. Measurement of passive membrane parameters with whole-cell recording from neurons in the intact amphibian retina. *J. Neurophysiol.* 61: 218–230, 1989.
- DACEY, D. M. AND LEE, B. B. The 'blue-on' opponent pathway in primate retina originates from a distinct bistratified ganglion cell type. *Nature* 367: 731–735, 1994.
- DARTNALL, H. J. The photosensitivities of visual pigments in the presence of hydroxylamine. *Vis. Res.* 8: 339–358, 1968.
- DIAMOND, J. S. AND COPENHAGEN, D. R. The relationship between light-evoked synaptic excitation and spiking behavior of salamander retinal ganglion cells. *J. Physiol. (Lond.)* 487: 711–725, 1995.
- DODGE, F. A., KNIGHT, B. W., AND TOYODA, J. Voltage noise in *Limulus* visual cells. *Science* 160: 88–90, 1968.
- FORTI, L., BOSSI, M., BERGAMASCHI, A., VILLA, A., AND MALGAROLI, A. Loose-patch recordings of single quanta at individual hippocampal synapses. *Nature* 388: 874–878, 1997.
- FREED, M. A., NELSON, R., STERLING, P., AND SMITH, R. Synaptic conductance for linear operation of ON-alpha ganglion cell. *Soc. Neurosci. Abstr.* 17: 344, 1991.
- FREED, M. A., PFLUG, R., KOLB, H., AND NELSON, R. ON-OFF amacrine cells in cat retina. *J. Comp. Neurol.* 364: 556–566, 1996.
- FREED, M. A., SMITH, R. G., AND STERLING, P. Computational model of the ON-alpha ganglion cell receptive field based on bipolar circuitry. *Proc. Natl. Acad. Sci. USA* 89: 236–240, 1992.
- FREED, M. A. AND STERLING, P. The ON-alpha ganglion cell of the cat retina and its presynaptic cell types. *J. Neurosci.* 8: 2303–2320, 1988.
- FRERKING, M. AND WILSON, M. Effects of variance in mini amplitude on stimulus-evoked release: a comparison of two models. *Biophys. J.* 70: 2078–2091, 1996.
- GAO, F., YANG, J. H., AND WU, S. M. Miniature inhibitory postsynaptic currents in retinal ganglion cells. *Invest. Ophthalmol. Vis. Sci. Suppl.* 38: 51, 1997.
- HAROSI, F. I. Absorption spectra and linear dichroism of some amphibian photoreceptors. *J. Gen. Physiol.* 66: 357–382, 1975.
- ISAACSON, J. S. AND WALMSLEY, B. Counting quanta: direct measurements of transmitter release at a central synapse. *Neuron* 15: 875–884, 1995.
- JENSEN, R. J. Intracellular recording of light responses from visually identified ganglion cells in the rabbit retina. *J. Neurosci. Methods* 40: 101–112, 1991.
- KATZ, B. AND MILEDI, R. The statistical nature of the acetylcholine potential and its molecular components. *J. Physiol. (Lond.)* 224: 665–669, 1972.
- KIER, C. K., BUCHSBAUM, G., AND STERLING, P. How retinal microcircuits scale for ganglion-cells of different size. *J. Neurosci.* 15: 7673–7683, 1995.
- KOCH, C., POGGIO, T., AND TORRE, V. Retinal ganglion cells: a functional interpretation of dendritic morphology. *Philos. Trans. R. Soc. Lond. B Biol. Sci.* 298: 227–264, 1982.
- KORN, H. AND FABER, D. Quantal analysis and synaptic efficacy in the CNS. *Trends Neurosci.* 14: 439–445, 1991.
- LAUGHLIN, S. The reliability of single neurons and circuit design: a case study. In: *The Computing Neuron*, edited by R. Durbin, C. Miall, and G. Mitchinson. New York: Addison-Wesley, 1989.
- LIU, G. AND TSIEN, R. W. Properties of synaptic transmission at single hippocampal synaptic boutons. *Nature* 375: 404–408, 1995.
- MARC, R. E., MURRY, R. F., AND BASINGER, S. F. Pattern recognition of amino acid signatures in retinal neurons. *J. Neurosci.* 15: 5106–5129, 1995.
- MARTIN, A. R. A further study of the statistical composition of the end-plate potential. *J. Physiol. (Lond.)* 130: 114–122, 1955.
- MASTRONARDE, D. N. Correlated firing of cat retinal ganglion cells. II. Responses of X- and Y-cells to single quantal events. *J. Neurophysiol.* 49: 325–349, 1983.
- MATSUI, K., HOSOI, N., AND TACHIBANA, M. Excitatory synaptic transmission in the inner retina: paired recordings of bipolar cells and neurons of the ganglion cell layer. *J. Neurophysiol.* 18: 4500–4510, 1998.
- MITTMAN, S., TAYLOR, W. R., AND COPENHAGEN, D. R. Concomitant activation of two types of glutamate receptor mediates excitation of salamander retinal ganglion cells. *J. Physiol. (Lond.)* 428: 175–197, 1990.
- NELSON, R., KOLB, H., ROBINSON, M. M., AND MARIANI, A. P. Neural circuitry of the cat retina: cone pathways to ganglion cells. *Vision Res.* 21: 1527–1536, 1981.
- PEICHL, L. AND WÄSSLE, H. Size, scatter and coverage of ganglion cell receptive field centres in the cat retina. *J. Physiol. (Lond.)* 291: 117–141, 1979.
- PFLUG, R., NELSON, R., AND AHNELT, P. K. Background-induced flicker enhancement in cat retinal horizontal cells. 1. Temporal and spectral properties. *J. Neurophysiol.* 64: 313–325, 1990.
- PROTTI, D. A., GERSCHENFELD, H. M., AND LLANO, I. GABAergic and glycinergic IPSCs in ganglion cells of rat retinal slices. *J. Neurosci.* 17: 6075–6085, 1997.
- RAASTAD, M., ENRIQUEZ-DENTON, M., AND KIEHN, O. Synaptic signaling in an active central network only moderately changes passive membrane properties. *Proc. Natl. Acad. Sci. USA* 95: 10251–10256, 1998.
- RAASTAD, M., JOHNSON, B. R., AND KIEHN, O. The number of postsynaptic currents necessary to produce locomotor-related cyclic information in neurons in the neonatal rat spinal cord. *Neuron* 17: 729–738, 1996.
- RALL, W. Branching dendritic trees and motoneuron membrane resistivity. *Exp. Neurol.* 1: 491–527, 1959.
- RAO, M. R., HARKINS, A. B., BUCHSBAUM, G., AND STERLING, P. Mammalian rod terminal: architecture of a binary synapse. *Neuron* 14: 561–569, 1995.
- RAO, R., BUCHSBAUM, G., AND STERLING, P. Rate of quantal transmitter release at the mammalian rod synapse. *Biophys. J.* 67: 57–63, 1994.

- RIEKE, F. AND SCHWARTZ, E. A. Asynchronous transmitter release: control of exocytosis and endocytosis at the salamander rod synapse. *J. Physiol. (Lond.)* 493: 1–8, 1996.
- SCHNEEWEIS, D. M. AND SCHNAPF, J. L. The photovoltage of macaque cone photoreceptors: adaptation, noise, and kinetics. *J. Neurosci.* 19: 1203–1216, 1999.
- SLAUGHTER, M. M. AND MILLER, R. F. 2-Amino-4-phosphonobutyric acid: a new pharmacological tool for retina research. *Science* 211: 182–184, 1981.
- STEINBERG, R. H. The distribution of rods and cones in the retina of the cat. *J. Comp. Neurol.* 148: 229–248, 1973.
- STEINBERG, R. H. AND WOOD, I. Pigment epithelial cell ensheathment of cone outer segments in the retina of the domestic cat. *Proc. R. Soc. Lond. B Biol. Sci.* 187: 461–478, 1974.
- STERLING, P. AND HARKINS, A. B. Ultrastructure of the cone pedicle in cat retina. *Invest. Ophthalmol. Vis. Sci. Suppl.* 31: 177, 1990.
- STRETTOI, E. AND MASLAND, R. H. The number of unidentified amacrine cells in the mammalian retina. *Proc. Natl. Acad. Sci. USA* 93: 14906–14911, 1996.
- TAYLOR, W. R., CHEN, E., AND COPENHAGEN, D. R. Characterization of spontaneous excitatory synaptic currents in salamander retinal ganglion cells. *J. Physiol. (Lond.)* 486: 207–221, 1995.
- TAYLOR, W. R., MITTMAN, S., AND COPENHAGEN, D. R. Passive electrical cable properties and synaptic excitation of tiger salamander retinal ganglion-cells. *Vis. Neurosci.* 13: 979–990, 1996.
- TEICH, M. C. Role of the double stochastic Neyman type-A and Thomas counting distributions in photon detection. *Appl. Opt.* 20: 2457–2467, 1981.
- TIAN, N., HWANG, T. N., AND COPENHAGEN, D. R. Analysis of excitatory and inhibitory spontaneous synaptic activity in mouse retinal ganglion cells. *J. Neurophysiol.* 80: 1327–1340, 1998.
- VELTE, T. J. AND MILLER, R. F. Dendritic integration in ganglion-cells of the mudpuppy retina. *Vis. Neurosci.* 12: 165–175, 1995.
- VON GERSDORFF, H., VARDI, E., MATTHEWS, G., AND STERLING, P. Evidence that vesicles on the synaptic ribbon of retinal bipolar neurons can be rapidly released. *Neuron* 16: 1221–1227, 1996.
- WALMSLEY, B., ALVAREZ, F. J., AND FYFFE, R.E.W. Diversity of structure and function at mammalian central synapses. *Trends Neurosci.* 21: 81–88, 1998.
- WONG, F. AND KNIGHT, B. W. Adapting bump model for eccentric cells of *Limulus*. *J. Gen. Physiol.* 76: 539–557, 1980.